

Katarzyna PIOTROWSKA^{a,*}, Monika MADEJ^a, Emil SPIŠÁK^b, Dariusz OZIMINA^a

^a Faculty of Mechatronics and Mechanical Engineering, Kielce University of Technology, Poland

^b Faculty of Mechanical Engineering, Technical University of Košice, Slovak Republic

* Corresponding author: kpawelec@tu.kielce.pl

INFLUENCE OF THE SURFACE ROUGHNESS OF Ti6Al7Nb ALLOY ON ITS BEHAVIOR IN BIOTRIBOLOGICAL SYSTEMS

© 2019 Katarzyna Piotrowska, Monika Madej, Emil Spišák, Dariusz Ozimina

This is an open access article licensed under the Creative Commons Attribution International License (CC BY)



<https://creativecommons.org/licenses/by/4.0/>

Key words: titanium alloys, SEM/EDS, biomaterials, friction, abrasive wear, contact angle, useful properties.

Abstract: The paper presents the results of studies of Ti6Al7Nb alloy properties used in biotribological systems. The following physicochemical treatments of the alloy were compared: polishing, sandblasting, etching as well as sandblasting and etching. Element identification was performed using a scanning electron microscope equipped with an EDS microanalyser. Scanning and confocal microscopy was used to observe surface morphology and topography. Frictional tests were carried out using a ball-disk coupling in reciprocating motion in technically dry friction and friction with lubrication with Ringer's solution. An optical tensiometer was used to determine the contact angle. As a result of the applied physicochemical treatments, surfaces of different morphology and geometric surface structure were obtained. The polished and etched sample had the most homogeneous surface. It was found that surface roughness significantly influences tribological properties. For the samples characterized by micro roughness of the surface, the best characteristics were obtained under conditions of technically dry friction. However, under the conditions of lubrication with Ringer's solution, the properties were the best for the samples characterized by nanoroughness. Ringer's solution reduced resistance to motion by approximately 20%. A negative influence of surface development on wetting was also found.

Wpływ chropowatości powierzchni na właściwości użytkowe stopu Ti6Al7Nb stosowanego w systemach biotribologicznych

Słowa kluczowe: stopy tytanu, SEM/EDS, struktura geometryczna powierzchni, tarcie, zużycie, kąt zwilżania, właściwości użytkowe.

Streszczenie: Przedstawiono wyniki badań właściwości stopu Ti6Al7Nb stosowanego w systemach biotribologicznych. Porównano ze sobą stop poddany następującym obróbkom fizykochemicznym: polerowaniu, piaskowaniu, trawieniu oraz piaskowaniu i trawieniu. Za pomocą mikroskopii skaningowej i konfokalnej obserwowano morfologię i topografię powierzchni. Identyfikację pierwiastków wykonano przy użyciu skaningowego mikroskopu elektronowego wyposażonego w mikroanalizator EDS. Badania tarcia zrealizowano w skojarzeniu kula–tarcza w ruchu posuwisto-zwrotnym w warunkach tarcia technicznie suchego oraz tarcia ze smarowaniem płynem Ringera. Do wyznaczenia kąta zwilżania wykorzystano tensjometr optyczny. W wyniku zastosowanych obróbek fizykochemicznych uzyskano powierzchnie o zróżnicowanej morfologii oraz strukturze geometrycznej powierzchni. Najbardziej jednorodną powierzchnią charakteryzowała się próbka polerowana oraz trawiona. Stwierdzono, że chropowatość powierzchni znacząco wpływa na właściwości tribologiczne. Dla próbek charakteryzujących się mikrochropowatością powierzchni uzyskano najlepsze charakterystyki w warunkach tarcia technicznie suchego. Natomiast w warunkach smarowania płynem Ringera były one najlepsze dla próbek wyróżniających się nanochropowatością. Płyn Ringera wpłynął na zmniejszenie oporów ruchu o około 20%. Wykazano również negatywny wpływ rozwinięcia powierzchni na zwilżalność.

Introduction

The surface texture of the outer layer determines the basic properties of materials used for producing medical implants. The first contact of the organism with the biomaterial occurs through the surface layer. The interaction between the surface of the implant and the biological environment *in vitro* or *in vivo* is related to the properties of the outer layer of the material, the most important of which are the following: chemical composition, topography, surface energy, and wetting [1–2].

The leading group of materials used for implants are metallic biomaterials. They are used for orthopaedic, dental, cardiac, and endovascular implants. Because they are in direct contact with tissues and bodily fluids, they have to meet strict requirements. The most important feature they should have is biocompatibility, i.e. the material's ability to behave properly in contact with tissue. The biocompatibility of implants depends on the physical structure of the material and its physicochemical properties in terms of the interaction with the biological system [3–5].

The most commonly used material in medical engineering is titanium and titanium alloys. It results from its functional properties, i.e. biocompatibility and good mechanical parameters (high strength and relatively low modulus of elasticity) [6–8]. The most popular is the $\alpha+\beta$ Ti6Al4V alloy. However, clinical observations on the biotolerance of this material indicate that vanadium ions are harmful. It has been proven to cause cytotoxic reactions and neurogenic disorders [9]. Therefore, a group of alloys of the second generation has been created, which include the Ti6Al7Nb alloy, among others. Vanadium is replaced by neutral niobium in this alloy. Chemical compositions of the oxide layer in both alloys are similar; however, Nb₂O₅ niobium oxides show greater biocompatibility and are less likely to dissolve in the environment of bodily fluids [10]. As a result of use, the oxide layer may be damaged and consequently lead to the release of metal ions, which are transported with blood and may enter into distant tissues [11]. Therefore, it is important that degradation products do not cause harmful reactions to the human body. In order to eliminate such hazards and improve the properties of titanium alloys, physicochemical treatments are applied. The surface can be modified using different methods depending on the planned effect. Medical implants, according to the development of their surface, can be divided into three groups: macro-, micro- and nanorough. Materials are described as micro-rough if the arithmetic mean deviation of the surface roughness S_a is between a few millimetres and a few tenths of micrometres. This type of topography allows only for mechanical anchoring of the implant in the bone, whereas large irregularities may hinder

cell growth [12]. For the S_a parameter equal to 1–10 μm (optimum value 1–2 μm), the surface is defined as micro-rough. It provides stability with a reduced risk of ion release. Nano-rough surfaces are defined as surfaces with S_a of less than 1 μm [13].

In case of orthopaedic and dental implants, an appropriate degree of surface roughness is desirable. Research on biomaterials has shown that osteoblasts develop better on surfaces with high surface development, but their division is faster than in the case of smooth surfaces [14]. Moreover, the developed topography of the surface of the implant increases the potential of biomechanical contact at the implant-bone tissue boundary, and it also influences the rate of protein adsorption and the healing process [15]. According to Wennerberg, implants with a medium roughness $S_a > 1\text{--}2\ \mu\text{m}$ cause faster bone tissue response compared to implants with a smooth $S_a < 0.5\ \mu\text{m}$ or more developed surface $S_a > 2\ \mu\text{m}$ [13]. The situation is completely different in the case of implants that come into direct contact with blood (e.g., stents). This type of implants requires the smallest possible development of surface texture, as blood cells quickly fill in microcavities on the surface of the implant [16]. The results of *in vivo* studies presented in [17] showing the reaction of the organism of farm animals to the development of the surface texture of the stent are noteworthy. It was shown that the topography of the surface of the implanted material affects the early and late reactions of the vessels with stents. In the case of unpolished surfaces, thrombosis occurred and the restenosis phenomenon, i.e. the recurrence of stenosis of the treated artery was more frequent. It was found that ensuring a smooth surface of stents is a basic stage in shaping their functional properties. Moreover, smooth surfaces promote colonization by fibroblasts, while surfaces with moderately developed surface topography cause the colonization and growth of osteoblasts by stimulating implant healing into bone tissue [15].

The article presents the use of various physicochemical surface treatments. As a result of polishing, sandblasting, etching, as well as sandblasting and etching, the samples of different morphology and surface texture were obtained. The applied treatments will be used to create surfaces in various implantological systems. As already noted, in the case of bone replacement implants, a faster osteointegration process will take place on surfaces with a moderate roughness. In the case of implants used in cardiac surgery, nanorough surfaces will be more useful.

1. Material and methodology

The materials used in the research were titanium discs with a diameter of 22 mm and a height of 6 mm with the mechanical properties presented in Table 1.

Table 1. Mechanical properties of Ti6Al7Nb alloy

Material	Young's modulus E [GPa]	Tensile strength R_m [MPa]	Compressive strength [MPa]	Hardness [Vickers]	Density [g/cm ³]
Ti6Al7Nb	105	1024	1074–1086	280–300	4.52

Table 2. Mechanical properties of aluminium(III) oxide

Material	Young's modulus E [GPa]	Tensile strength R_m [MPa]	Compressive strength [MPa]	Hardness [Vickers]	Density [g/cm ³]
Al ₂ O ₃	393	206–300	2070–2620	1365	3.987

The material that constituted a countersample in the tribological tests were balls made of aluminium oxide (III) – Al₂O₃, with diameters equal to 6 mm and a surface roughness S_a equal to 0.37 μm which was loaded with a normal force equal to 5 N. The most important mechanical properties of Al₂O₃ are shown in Table 2.

The faces of the discs were mechanically sanded with Buehler's Automet 250 grinder-polisher. SiC sandpapers with increasing grain gradations ranging from 120 to 2500 were used. The surfaces of the discs were then polished using polishing cloths and diamond pastes with grain sizes of 6 μm , 1 μm , and 0.05 μm . The aim of the treatment was to even out the surface before performing physicochemical treatments (sandblasting, etching, and sandblasting and etching). It was assumed that the polished surface was a reference sample. Sanding was carried out with a Wasserman sandblaster using Cobra Al₂O₃ abrasive with a gradation of 125 μm . After abrasive blasting, the discs are washed in distilled water and then in ethanol in an ultrasonic cleaner for 5 minutes each time. The surfaces of the discs were then dried using compressed air. The next step was to etch both polished and sandblasted samples. The aim of etching was to reveal the microstructure of the sample, i.e. the

shape and size of grains. The etching time pick was 2 minutes. The process took place in a solution consisting of 20 mL HF, 10 mL HNO₃, and 20 mL glycerine. In the final phase, the discs were subjected to the following tests: surface morphology, surface texture, tribological tests, and the determination of the contact angle.

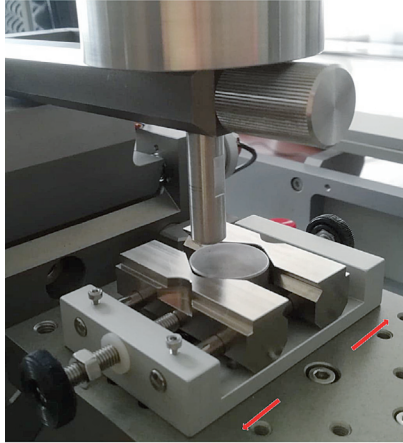
Observations of the morphology and the determination of chemical composition were carried out using the Phenom XL scanning microscope, equipped with **an integrated energy dispersive spectrometer – EDS**. Analyses of the surface texture before and after tribological tests were performed on a Leica DCM8 confocal microscope with an interferometry mode. Experimental tribological tests were carried out on a TRB³ pin-on-disc tribometer in reciprocal motion. A photograph of the friction node is shown in Figure 1. The tribological tests were carried out with the technical and environmental parameters presented in Table 3. Resistance to motion was determined during technically dry friction (TDF) and with the use of Ringer's solution (RS) as a lubricant. The chemical composition of the solution used is shown in Table 4. The tribological tests were repeated 5 times for each friction pair at the set parameters.

Table 3. Technical and environmental parameters of test

Friction pair	Unit	Tribometer TRB ³
		Al ₂ O ₃ ball Φ 6 mm – disc Ti6Al7Nb Φ 22 mm
Load	N	5
Sliding velocity	m/s	0.0159
Cycle	–	5000
Frequency	Hz	1
Humidity	%	40 \pm 5
Temperature	$^{\circ}\text{C}$	23 \pm 1

Table 4. Chemical composition of Ringer's solutions pH 5.1 (1000 mL)

Chemical composition [g]		
NaCl	KCl	CaCl ₂
8.60	0.30	0.48

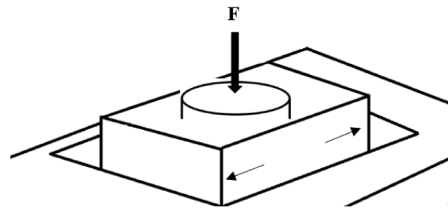
**Fig. 1. View of pin-on-disc**

Contact angle measurements were performed using an Attension Theta tensiometer. The static contact angle was determined during the tests, consisting in precise placement of drops of selected measuring liquids with a volume of approx. 4 μ L on the tested surface and immediate measurement. Distilled water (pH 7) and Ringer's solution (pH 5.1) were used in the tests. The photograph of drops was taken with a digital camera after 2 seconds from the moment when it was placed on the surface of the sample. The drops were applied to each disc in a different part of the sample each time. The measurement was repeated 6 times. The contact angle was determined using OneAttension software on the basis of the measurement of the geometry of a drop of a measuring liquid applied to a given surface.

2. Result and discussion

The aim of the research conducted using scanning electron microscopy (SEM) was a three-dimensional analysis of the surface morphology of the tested samples (Fig. 2) and quantitative analysis of the chemical composition in microscale (Table 5).

The surface morphology analysis showed that the polished sample has the most homogeneous surface. As a result of sandblasting, the surface of the titanium alloy had typical features for abrasive blasting, i.e. matte, heterogeneous, and developed, with high surface roughness. Visible pores with a diameter of about 1.02 μ m were observed on the samples subjected to etching. The surface of a titanium alloy sandblasted with aluminium



oxide and then etched also had a homogeneous surface with less roughness than that of a sample which was only sandblasted.

Table 5 presents the elemental composition of the tested samples obtained from the EDS analysis. This is the average of 10 measurements. The values are given as weighted percentages. All test samples consist predominantly of titanium. There is also a relatively large amount of oxygen in the form of an oxide layer formed spontaneously on the surface of titanium as a result of contact with atmospheric air. The presence of aluminium was observed in all tested samples. This element is both part of the alloy and the powder used in the sandblasting process. The etching process caused the exposure of niobium grains. The content of niobium in the etched sample is approximately 50% higher than in the other tested discs.

The next stage of the research was the assessment of the surface texture after polishing, sandblasting, and etching. Figures 3 and 4 show isometric images and distributions of the ordinates of surfaces with Abbott-Firestone curves. Additional information on the shape of the surface was obtained from amplitude parameters (Table 6).

The three-dimensional images made it possible to analyse and understand the geometric structure of the samples after polishing, sandblasting, and etching. Knowledge of the geometry of a surface is very useful when assessing its functional properties. The results of the tests revealed that, after sandblasting, and sandblasting and etching, the disc had the most developed surface texture.

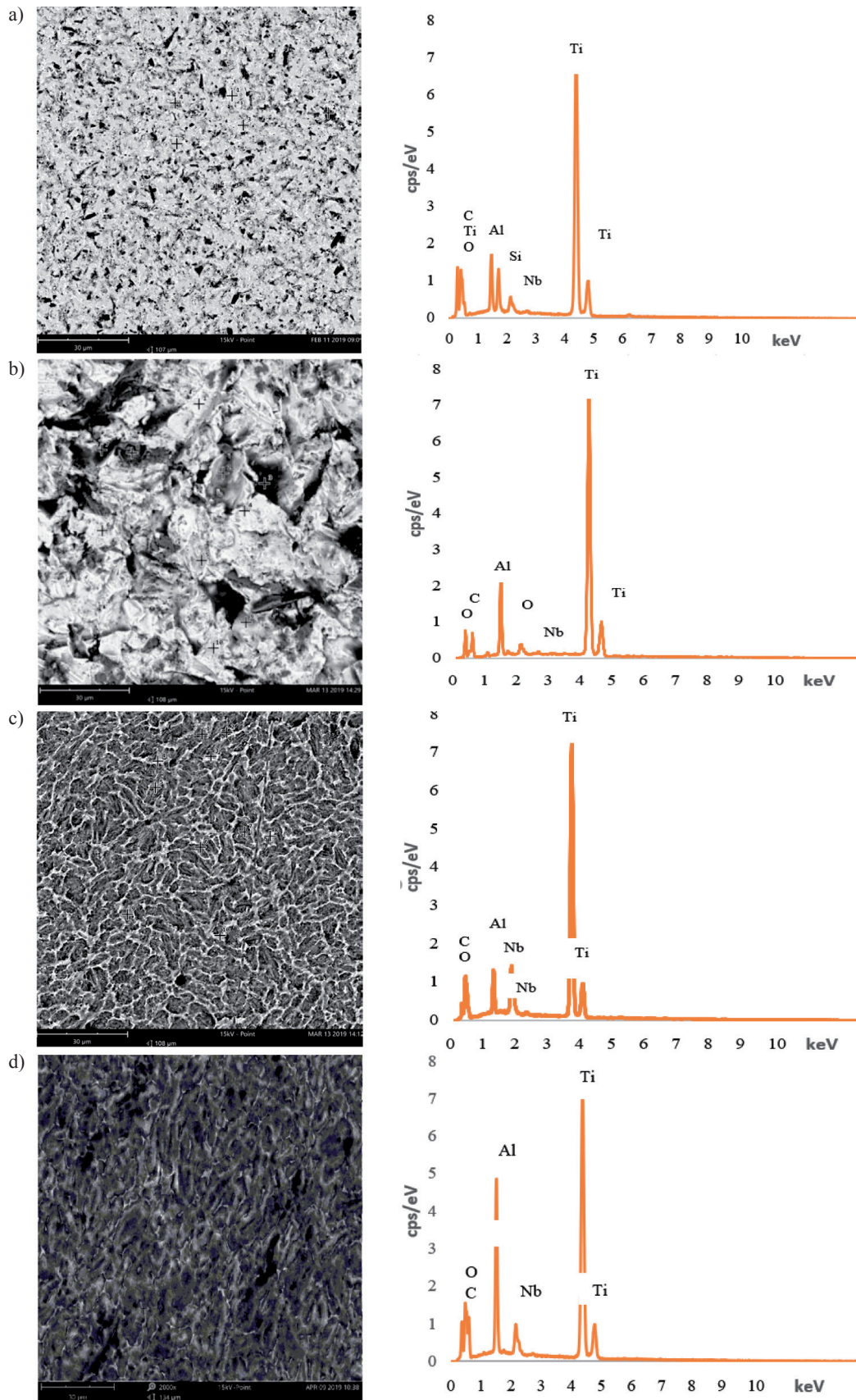


Fig. 2. SEM images and exemplary spectrum analyses of the chemical composition Ti6Al7Nb alloy: a) polished, b) sandblasted, c) etched, d) sandblasted and etched

Table 5. Chemical composition of titanium alloy after physicochemical treatments

Weight [%]	Ti	O	Al	Nb	Si	C
Polished	65.8	7.6	4.4	6.8	1.6	13.2
Sandblasted	64.1	14.4	7.1	5.7	0.2	9.0
Etched	65.7	13.7	4.2	10.9	–	5.4
Sandblasted and etched	68.5	16.1	7.9	5.5	–	2.0

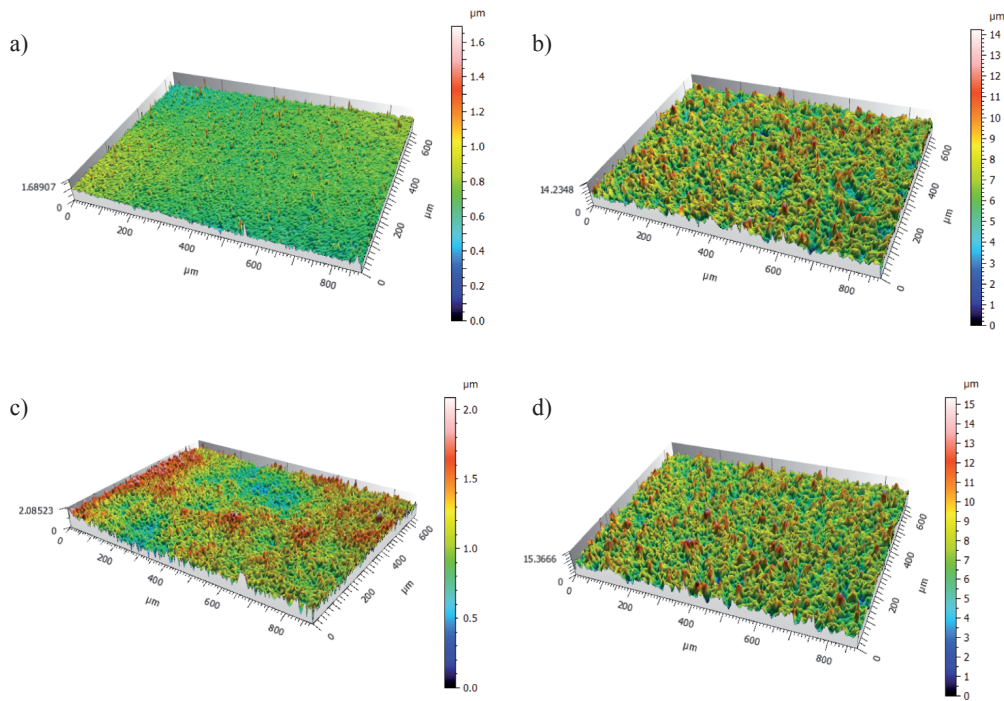


Fig. 3. The isometric image of Ti6Al7Nb: a) polished, b) sandblasted, c) etched, d) sandblasted and etched

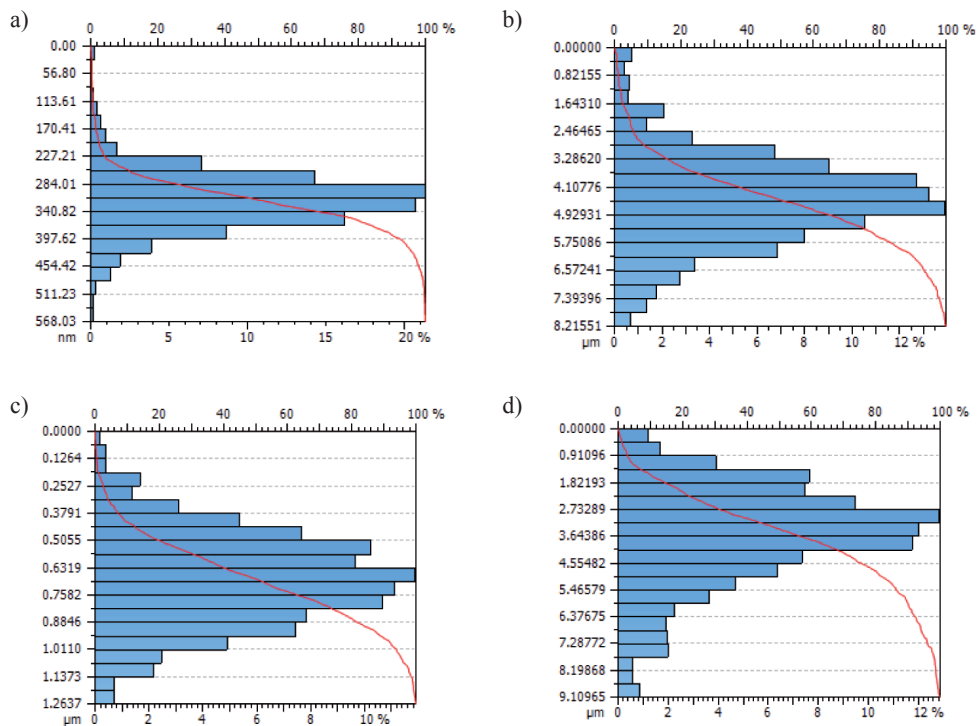


Fig. 4. Ordinate distribution and Abbott – Firestone curve: a) polished, b) sandblasted, c) etched, d) sandblasted and etched

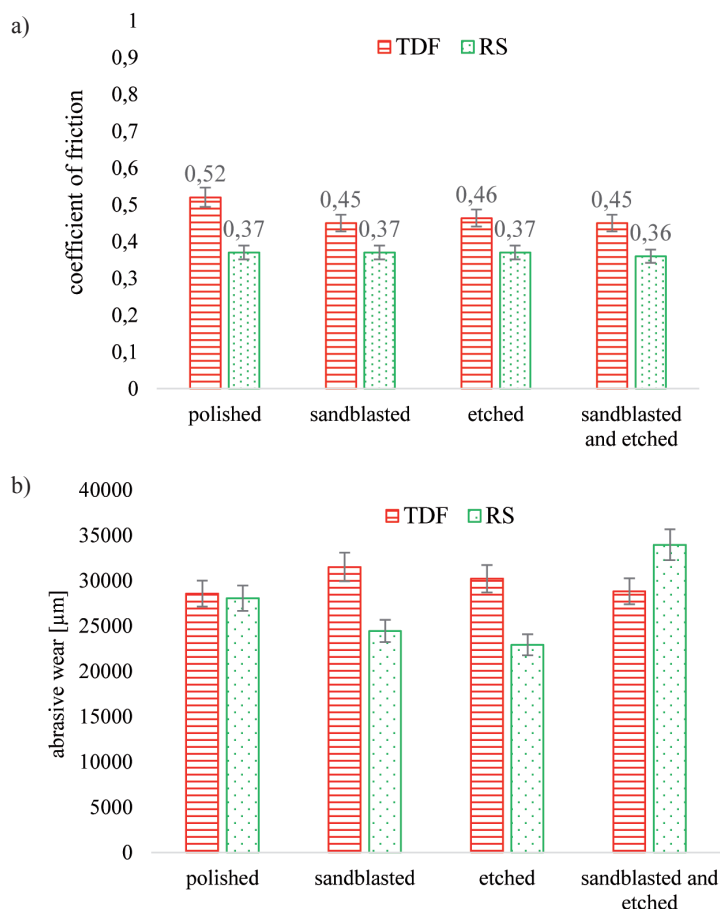
Table 6. Parameters of the surface texture

Parameter	Specification	Polished	Sandblasted	Etched	Sandblasted and etched
S_a [μm]	Arithmetical mean height of surface	0.0667	1.2369	0.2342	1.4266
S_p [μm]	Maximum surface peak height	0.9610	7.4563	1.0517	8.0566
S_v [μm]	Maximum depth of surface	0.7280	6.7784	1.0335	7.3099
S_z [μm]	Maximum height of surface	1.6890	14.2348	2.0852	15.366
S_{sk}	Skewness of surface	0.6972	0.1218	0.0940	0.0366
S_{ku}	Kurtosis of surface	9.7005	3.4955	3.1026	3.6842

Additional information about the state of the outer layer can be read from the amplitude parameters: skewness (S_{sk}) and kurtosis (S_{ku}). The coefficient of asymmetry S_{sk} , called *skewness*, characterizes the symmetry of the distribution of ordinates of roughness height in relation to the mean plane. This parameter is sensitive to any changes in the shape of the surface. A positive value of this coefficient indicates a surface with elevations in a sharpened shape. Table 6 indicates that, in all cases, S_{sk} takes positive values. Kurtosis, or the *coefficient of concentration*, is a measure of the smoothness of the distribution curve of profile ordinates. The S_{ku} value of 3 indicates that the ordinate curve of

the roughness profile is close to normal distribution [18]. Table 6 shows that, in three out of four analysed samples, the S_{ku} value takes a value close to 3. However, when analysing the ordinate distributions, it was noticed that only on the sandblasted surface are the distribution of the ordinates of the roughness profile close to normal distribution.

In the next stage, tribological tests were performed. Figure 5 shows the average friction coefficients and abrasive wear recorded during the tests in the technically dry friction conditions and in the conditions of friction with lubrication using the Ringer's solution.

**Fig. 5. Coefficient of friction (a), abrasive wear (b)**

The results of tribological tests revealed that the nature of the outer layer has little influence on the value of the coefficient of friction (μ). The values of the coefficients of friction were comparable for all tested samples. The value of μ parameter oscillated between 0.45–0.52 for technically dry friction and 0.36–0.37 for friction using a lubricant. The lowest coefficients of friction in all tests were obtained for sandblasted and etched specimens. The lubricant used reduced the resistance to motion in all the tested cases.

After the tribological tests were finished, the traces of wear were measured on the samples. The measure of consumption was the maximum depth and the surface area of the wear on the cross-section. Figures 6–7 show the isometric images and the wear profiles of the tested samples.

Tests performed with an optical profilometer revealed that both technically dry friction and friction using Ringer's solution as lubrication resulted in even wear of the surface layer. Analysis of the geometric structure after tribological tests carried out under technically dry friction conditions indicates that the material with the least wear in the friction pair with the aluminium oxide ball was polished titanium. The area of wear was about 10% smaller than the other discs. Tests using Ringer's solution have shown a reduction in wear in most cases. The best characteristics were obtained for the etched sample. The exception was the sandblasted and etched sample. For this sample, the lowest friction coefficients and a 15% increase in wear were recorded in comparison with technically dry friction. On the basis of friction tests, it was found that the best tribological characteristics were obtained for nanorough samples.

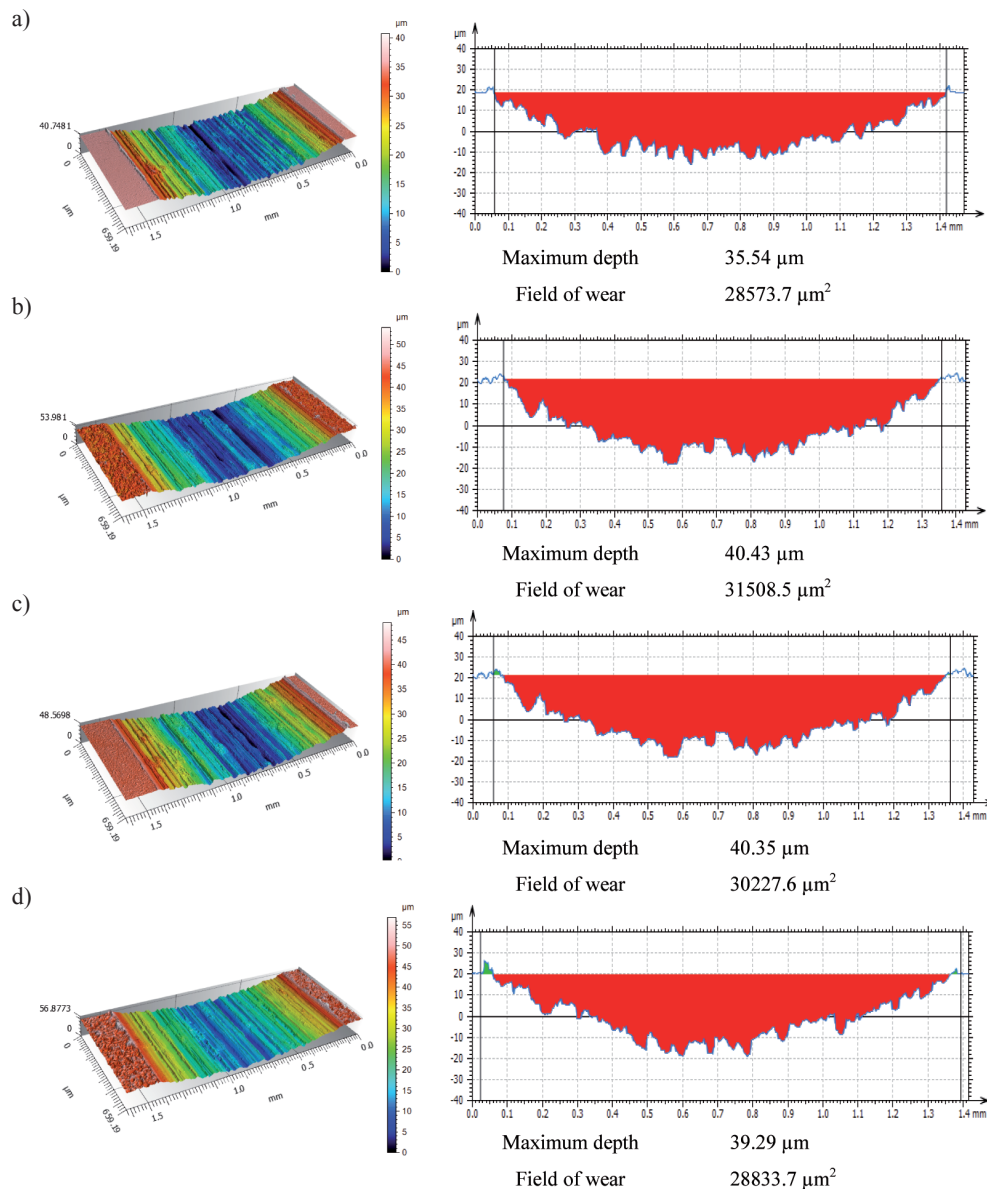


Fig. 6. The isometric image of the trace of wear and the wear profile in a cross-section for technically dry friction: a) polished, b) sandblasted, c) etched, d) sandblasted and etched

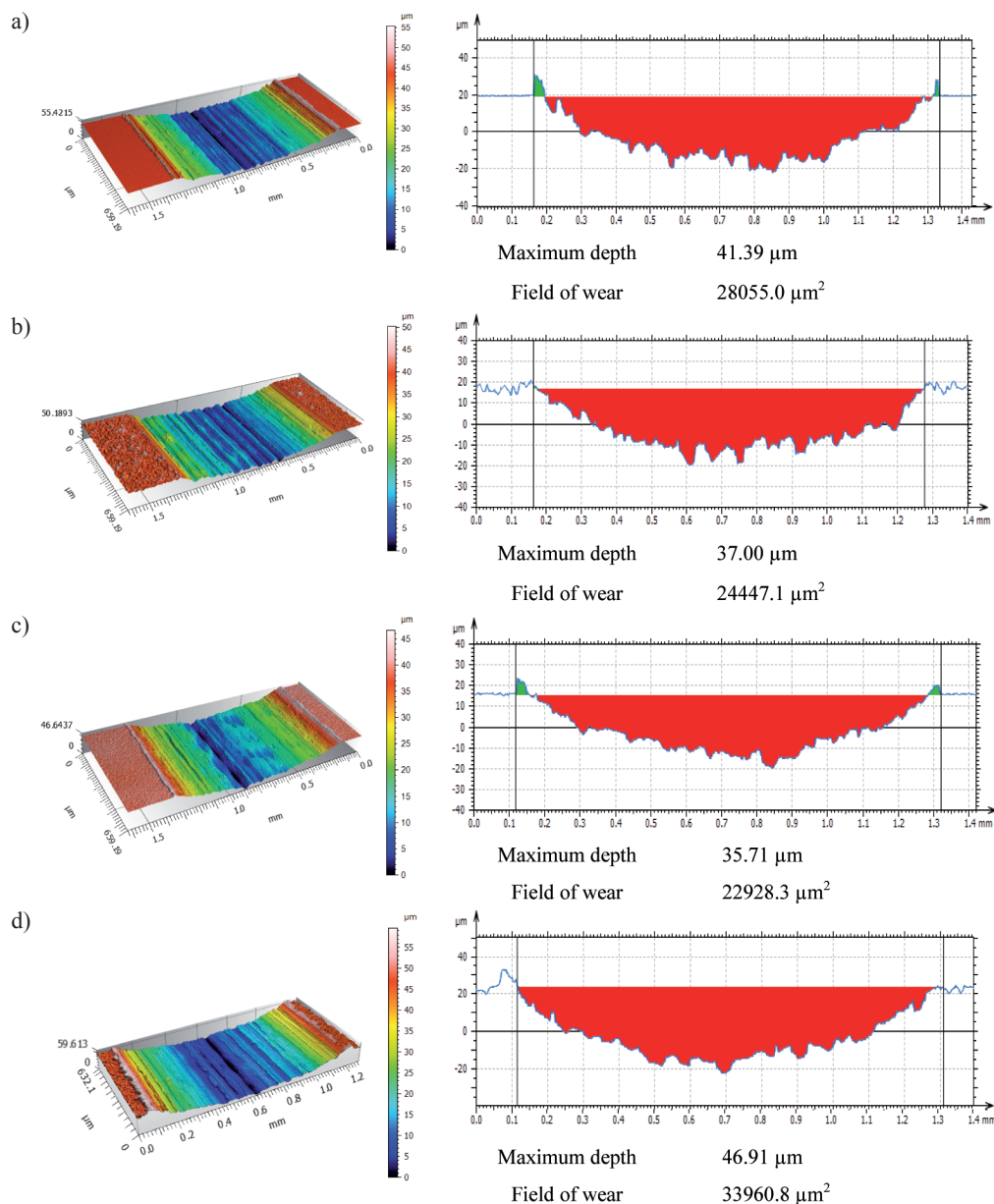


Fig. 7. The isometric image of the trace of wear and the wear profile in a cross-section on the conditions lubrication the Ringer's solution: a) polished, b) sandblasted, c) etched, d) sandblasted and etched

The next stage consisted in determining the wettability of the surface using distilled water and Ringer's solution. Figure 8 presents an example of the contact angles of the tested surfaces for Ringer's solution. Mean values of the recorded contact angles for the applied measuring liquids are shown in Fig. 9.

Measurements of surface wetting are extremely important when assessing the adhesion of cells to the implant surface. It is a well-known fact that the adhesion of cells decreases on hydrophobic surfaces and increases on hydrophilic surfaces [19–20]. The osseointegration mechanism starts when the implant gets in contact with the blood. To increase the implant surface area for human osteoblast adhesion, it is necessary to increase

the surface wettability. Measurements of the contact angle confirmed the development of the geometric structure affecting wetting. The contact angle values presented in Fig. 9 show that two of the four analysed samples are hydrophilic. The lowest contact angle values for all analysed liquids were observed on polished surfaces; they were about 20% lower in comparison with the remaining samples. In the case of surfaces after sandblasting and etching (with a very developed surface texture), the highest contact angle values were recorded for all applied measuring liquids. Therefore, the titanium alloy subjected to sandblasting and etching is characterized by the worst wetting.

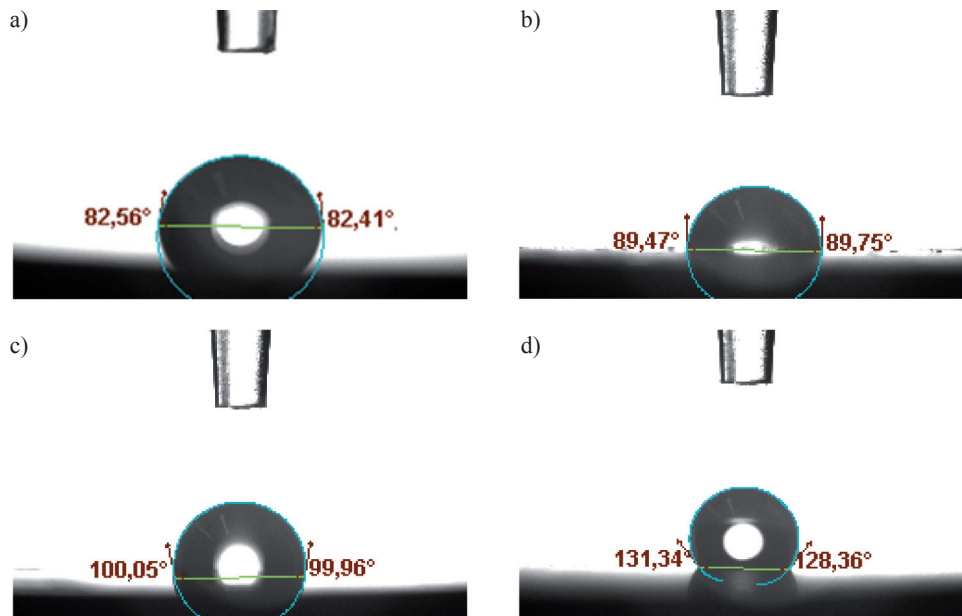


Fig. 8. The photo of the Ringer's solutions: a) polished, b) sandblasted, c) etched, d) sandblasted and etched

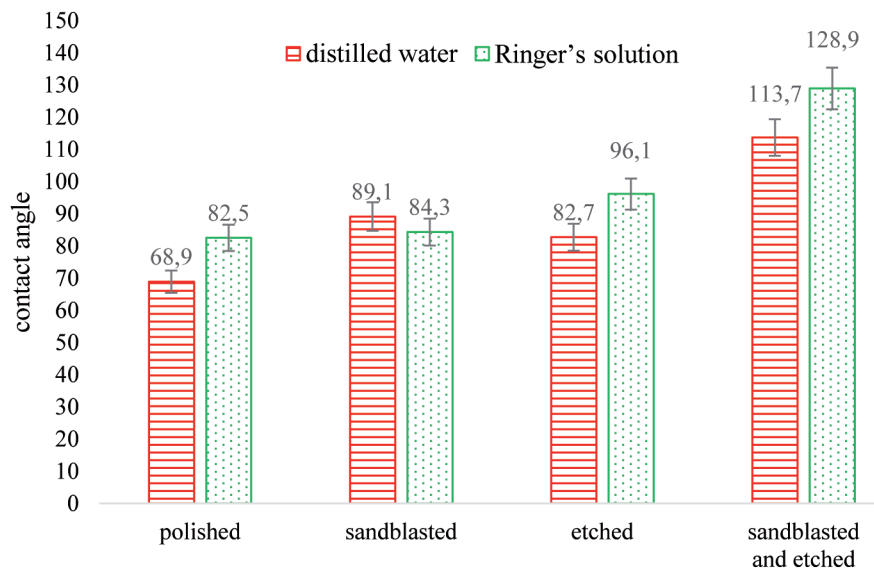


Fig. 9. Medium contact angle of Ti6Al7Nb surfaces

Conclusions

As a result of the conducted research, the following final conclusions were drawn. Microscopic observations showed that the analysed surfaces are characterized by different morphology, depending on the type of applied physicochemical treatment. On the basis of chemical composition analysis, it was found that all the tested samples consisted mainly of titanium and the etching process caused the exposure of niobium

grains. Measurements of the geometric structure of the surface revealed that discs subjected to sanding as well as sanding and etching have higher surface roughness parameters compared to polished and etched discs. The results of tribological tests showed that the geometric structure of the surface has little influence on the value of the coefficient of friction and, with the used lubricant, reduces the resistance to motion. The lowest values of the coefficients of friction were obtained for the sample with the highest roughness. Tests performed with

a confocal microscope showed that both technically dry friction and friction using Ringer's solution as lubrication resulted in even wear of the surface layer. Although the least resistance to motion was achieved for the sandblasted and etched sample, the analysis of wear revealed that it was the highest. When analysing the results of the geometric structure of the surface after tribological tests, the lowest wear was found for nanorough samples. The results of contact angle tests have shown that surfaces with developed topography have the lowest wetting. For a deeper analysis of the influence of surface development on the properties of Ti6Al7Nb, the scope of the research should be extended to include corrosion and microbiological tests, which will be a further stage of the research.

References

1. Kneć-Liber A., Łagan S.: The Use of Contact Angle and the Surface Free Energy as the surface characteristics of the Polymers used in medicine. *Polim. Med*, 2014, 1(44), pp. 29–37.
2. Bartolomeu F., Costa M.M., Gomes J.R., Alves N., Abreu C.S., Silva F.A., Miranda G.: Implant surface design for improved implant stability – A study on Ti6Al4V dense and cellular structures produced by Selective Laser Melting. *Tribology International*, 2019, 129, pp. 272–283.
3. Przybyszewska-Doroś I., Okrój W., Walkowiak B.: Surface modifications of metallic implants. *Engineering of Biomaterials*, 2005, 43–44, pp. 52–62.
4. Madej M.: *Properties of tribological systems with diamond-like carbon coatings*. Kielce: Ed. TU, 2013.
5. Ozimina D., Ryniewicz A.: *Exploitation of tribological systems*. M48, tome I. Kielce: Wyd. PŚk, 2013.
6. Pawelec K., Madej M., Baranowicz P., Wysokińska-Miszczuk J.: Influence of pH on the tribological properties of DLC – coated Ti-6Al-4V titanium alloy: *AIP Conference Proceedings*, 2018, 2017, 020021.
7. Łukaszewska M., Gajdus P., Hędzerek W., Zagalak R.: Development of titanium implants surface. Review. *Implantoprosthesis*, 2009, X, 3, pp. 24–29.
8. Ganesh B.K.C., Ramanaiah N., Chandrasekhar Rao P.V.: Effect of Surface Treatment on Tribological Behavior of Ti-6Al-4V Implant Alloy. *Journal of Minerals and Materials Characterization and Engineering*, 2012, 11, pp. 735–743.
9. Zasińska K.: *The influence of ion implantation on the selected utility properties of the Ti-13Nb-13Zr alloy in aspect of application on a friction elements in a hip joint endoprostheses*. [PhD thesis]. Gdańsk University of Technology, 2017 [in Polish].
10. Dąbrowski R., Pacyna J., Kochańczyk J.: The formation of microstructure and fracture toughness of Ti6Al7Nb alloy for biomedical applications. *Acta Bio-Optica et Informatica Medica. Inżynieria Biomedyczna*, 2016, 22(3), pp. 130–137.
11. Blumenthal N.C, Cosma V.: Inhibition of apatite formation by titanium and vanadium ions. *J Biomed Mater Res*, 1989, 23, pp. 13–22.
12. Vandrovcová M. Bačáková L.: Adhesion, Growth and Differentiation of Osteoblasts on Surface-Modified Materials Developed for Bone Implants. *Physiol Res*, 2011, 60, pp. 403–417.
13. Łukaszewska-Kuska M.: *Evaluation of osteoblasts potential in the osseointegration process on variously modified titanium surfaces. In vitro studies*. [PhD thesis]. Poznan University of Medical Sciences, 2013 [in Polish].
14. Nowacka M.: Biomaterials for tissue engineering and regenerative medicine. *Wiadomości Chemiczne*, 2012, 66, pp. 911–933.
15. Piotrowska K., Madej M., Baranowicz P., Wysokińska-Miszczuk J., Skóra M.: The tribological properties of the Ti6Al4V alloy by nitrogen ions. *Bimonthly Tribologia*, 2019, 1, pp. 37–49.
16. Martini D., Fini M., Franchi M., Pasquale V.D., Bacchelli B., Gamberini M., Tinti A., Taddei P., Giavaresi G., Ottani V., Raspanti M., Guizzardi S., Ruggeri A.: Detachment of titanium and fluorohydroxyapatite particles in unloaded endosseous implants. *Biomaterials*, 2003, 24, pp. 1309–1316.
17. Paszenda Z.: *Shaping physicochemical properties of Co-Ni-Mo coronary stents for applications in surgical cardiology*. Gliwice: Silesian University of Technology, 1997.
18. Milewski K., Madej M., Niemczewska-Wójcik M., Ozimina D.: Evaluation of the properties of diamond-like carboncoatings lubricated with ionic liquids. *Tribologia*, 2017, 5, pp. 37–46.
19. Roach P., Eglin D., Ronde K., Perry C.C., Mater J.: Modern biomaterials: a review – bulk properties and implications of surface modifications. *Sci.: Mater. Med.*, 2007, 18(7), pp. 1263–1277.
20. Roach P., Parker T., Alexander M.R., Gadegaard N.: Surface strategies for control of neuronal cell adhesion: A review. *Surface Science Reports*, 2010, 65(6), pp. 145–173.

This article appeared in its printed version in Journal of Machine Construction and Maintenance. The electronic version is published in DEStech Publications, Inc., Lancaster, PA, 2019, Proceedings of FUTURE ENGINEERING CONFERENCE.